

# การศึกษาเชิงทฤษฎีของสมบัติเชิงโครงสร้างและสมบัติเชิงอิเล็กทรอนิกส์ของคาร์บอนนาโนแคปที่โดปด้วยโลหะทรานซิชันแถวแรก

## Theoretical investigation of structural and electronic properties of the first row transition metal-doped on carbon nanocaps

สุทธิพงษ์ โฮมพาน,<sup>1</sup> ณัฐฐาเนตร นันทบุต, <sup>2</sup> บรรจบ วันโน <sup>2\*</sup>  
Suttipong Hompan,<sup>1</sup> Nadtanet Nunthaboot,<sup>2</sup> Banchob Wannoo <sup>2\*</sup>

### บทคัดย่อ

ในงานวิจัยนี้ได้ศึกษาสมบัติเชิงโครงสร้าง พลังงาน การถ่ายโอนประจุ และสมบัติเชิงอิเล็กทรอนิกส์ ของคาร์บอนนาโนแคปที่โดปด้วยโลหะทรานซิชันคือ สแกนเดียมไทเทเนียมวานาเดียมโครเมียมและแมงกานีส ศึกษาด้วยวิธีทฤษฎีฟังก์ชันความหนาแน่น ผลการคำนวณแสดงให้เห็นว่าหลังการโดปด้วยโลหะเหล่านี้ โครงรูปของคาร์บอนนาโนแคปเกิดการเปลี่ยนแปลงขึ้นอย่างชัดเจน ที่บริเวณตำแหน่งที่ทำการโดป ซึ่งมีรูปร่างคล้ายพีระมิด เมื่อพิจารณาความสามารถในการยึดจับของโลหะกับคาร์บอนนาโนแคป พบว่าไทเทเนียมอะตอมเกิดอันตรกิริยาที่แข็งแรงที่สุดในขณะที่สแกนเดียมอะตอมเกิดอันตรกิริยาได้อ่อนที่สุด กับคาร์บอนนาโนแคปนอกจากนี้งานวิจัยนี้ยังได้รายงานถึงออบิทัลเชิงโมเลกุล พลังงานออบิทัลและความหนาแน่นสภาวะของคาร์บอนนาโนแคปที่โดปด้วยโลหะเหล่านี้ด้วย

**คำสำคัญ:** คาร์บอนนาโนแคป ทฤษฎีดีเอฟที โลหะทรานซิชัน สมบัติเชิงโครงสร้าง สมบัติเชิงอิเล็กทรอนิกส์

### Abstract

The structure, energy, charge transfer, and electronic properties of carbon nanocap (CNC) doping with the first row transition metals, i.e., Sc, Ti, V, Cr, and Mn atoms were studied using the density functional theory method. Calculated results showed that after doped with those metal ions, the geometrical structures of the CNC dramatically change at the doping site to form the pyramidal shape. The binding ability indicated that Ti and Sc atoms exhibited the strongest and the weakest interactions with CNC. In addition, frontier molecular orbitals, orbital energies, and density of states of TM-doped CNC were also reported.

**Keywords:** Carbon nanocap, DFT, Transition metals, Structural property, Electronic property

<sup>1</sup> นิสิตปริญญาโท, สาขาเคมีศึกษา คณะวิทยาศาสตร์ มหาวิทยาลัยมหาสารคาม อำเภอกันทรวิชัย จังหวัดมหาสารคาม 44150

<sup>2</sup> อาจารย์, ศูนย์ความเป็นเลิศทางด้านนวัตกรรมทางเคมีและหน่วยวิจัยเคมีซูปราโมเลกุล ภาควิชาเคมี, คณะวิทยาศาสตร์ มหาวิทยาลัยมหาสารคาม อำเภอกันทรวิชัย จังหวัดมหาสารคาม 44150

<sup>1</sup> Graduate student, Department of Chemistry Education, Faculty of Science, Mahasarakham University, Kantharawichai, MahaSarakhm 44150, Thailand.

<sup>2</sup> Lecturer, Center of Excellence for Innovation in Chemistry and Supramolecular Chemistry Research Unit, Department of Chemistry, Faculty of Science, Mahasarakham University, Kantharawichai, MahaSarakhm 44150, Thailand.

\* Corresponding author: BanchobWannoo, Center of Excellence for Innovation in Chemistry and Supramolecular Chemistry Research Unit, Department of Chemistry, Faculty of Science, Mahasarakham University, Kantharawichai, MahaSarakhm 44150, Thailand.

## Introduction

A lot of research topics are concentrated on some properties of carbon-based nanostructures. It is well known that their structures are shown outstanding chemical and physical properties depending on their large specific area and lightweight. Carbon nanotube (CNT) is a new kind of nanostructures, which was established since in 1991 by using carbon arc-discharge evaporation method.<sup>1</sup> Single-walled carbon nanotube (SWCNT) is expected to be good candidates for the promising materials in the future. Since the electronic structure of SWCNTs depends on geometrical structure and chirality, SWCNTs can be typically metallic or semiconducting.<sup>2</sup> Therefore, they have been attracted significant attention over the past few years. Due to excellence properties, their applications in materials science and nanotechnology fields were widely studied.<sup>3</sup> The large potential technological applications of sensors, storage materials, and electronics were reviewed.<sup>4-6</sup> In particular, many researches focus on a new typical sensor from the viewpoint of modified surface nanomaterials.

In the case of sensor applications, a good example obtained in this class known as sidewall modification with free metals has been achieved to improve their electronic properties. Up until now, doping elements onto the sidewall surface reactivity and the tip of the tube is interestingly challenged. Surface modifications of CNTs by doping metals were found to significantly enhance the surface reactivity which were widely used as substrate to small gas adsorption.<sup>4,7,8</sup>

Especially, the closely related transition metals (TMs)-doped SWCNTs have been reported. Decorating of atomic TMs on SWCNTs or related carbon frameworks has been studied using the density functional theory (DFT)

calculations.<sup>9,10</sup> Interestingly, TM-doped carbon frameworks (e.g., bucky bowls, fullerenes, and nanotubes) have been investigated under the DFT method.<sup>11</sup> These results suggested that TM-doped nanotubes may offer opportunities to achieve complementary selectivity in comparison to traditional Lewis acid catalysts. In addition, their structures interacted with a dopant TM atom are exhibited and imparted additional stability to these otherwise highly reactive. In a similar way, TM atoms doped on surface of SWCNTs with both exo and endo doping configurations have been studied within DFT method.<sup>10</sup> In the results, the geometric and electronic properties of these TM-doped SWCNTs are much changed and exhibited to enhancements and improvements in selectivity.

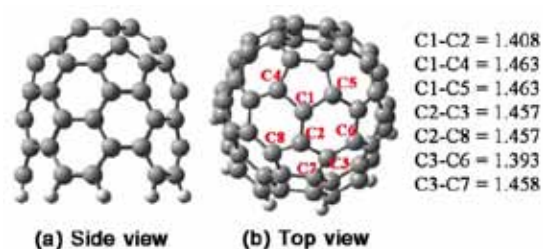


**Figure 1.** Optimized/modeled structures of a pristine CNC (a) side view and (b) top view with doping configuration sites for various transition metal doped structures. The modeled doping configuration sites are presented in the letter, namely C1, C2, and C3 for doping configuration systems. The bond lengths are presented in Å.

Many works have previously reported that synthesis of carbon frameworks are based on chemical vapor deposition method. Opened fullerene is generated a new type of carbon nanotube, they called the capped single-walled carbon nanotube.<sup>12</sup> Due to the strong catalytic activity of the transition metal, a new material doped with TM atom that could possibly be used in the field of sensor applications has been

designed. In this research, the geometrical, charge transfer, and electronic properties of single-walled carbon nanocap (CNC) and the first row TMs-doped CNCs have been investigated using the DFT.

## Computational details

### Geometry optimizations

To obtain the most stable structures, all of calculations were carried out using the Gaussian 09 computational package<sup>13</sup> and DFT method. Based on the spin-restricted Kohn-Sham equation, these methods were solved for estimating the electronic structure. A hybrid density functional B3LYP, Becke's three parameter exchange functional with the Lee-Yang-Parr correlation functional was used to approximate the exchange-correlation interactions.<sup>14,15</sup> The electronic wave functions were expanded in the Los Alamos LanL2DZ split-valence basis set with the core shell electrons represented by the LanL2 effective core potentials.<sup>16</sup> As in Figure 1, capped single-walled carbon nanotube, compose of 60 carbon atoms with hydrogen atoms to saturate dangling bonds, was used as model of the CNC. Doping atoms with the first row TM (Sc, Ti, V, Cr, and Mn) on the CNC were considered. The labeled positions C1, C2, and C3 (see Figure 1b) were replaced by one of a TM atom. Therefore, the systems of TM-doped onto CNC with each position were called TM-CNC(C1), TM-CNC(C2), and TM-CNC(C3).

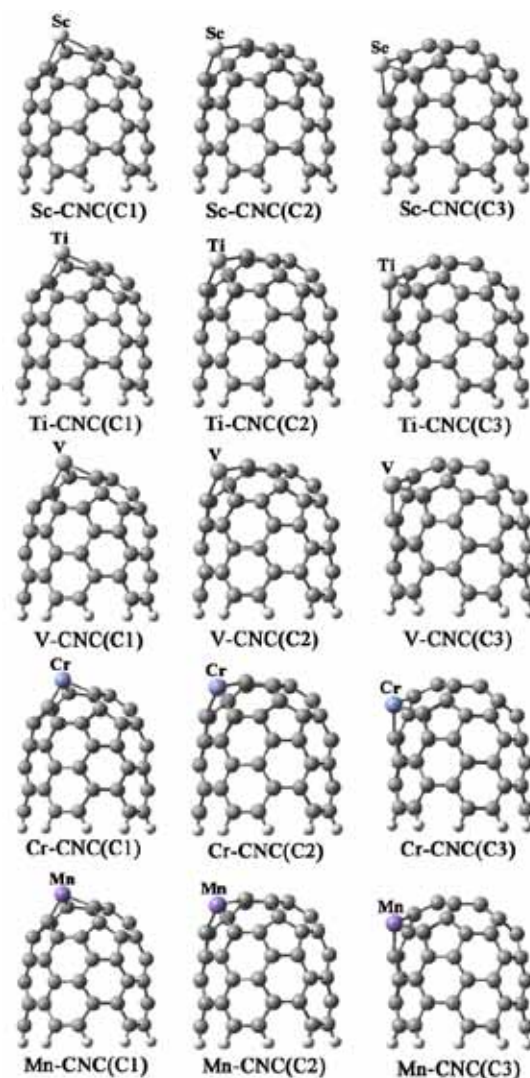


**Figure 2.** . The Optimized structures of transition-doped CNC at the various doping configuration sites as computed at the B3LYP/LanL2DZ level.

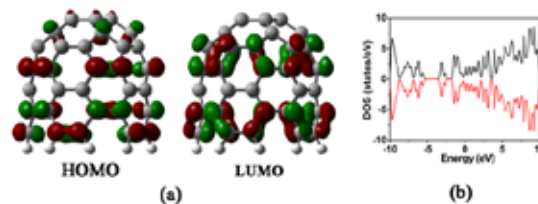


**Figure 3.** (a) The frontier molecular orbitals and (b) density of states (DOS) of pristine CNC.

### Binding energies

The binding energies ( $E_b$ ) of CNCdoped with a TM atom at the difference sites were calculated as equation:

$$E_b = E_{TM-CNC} - E_{CNC} - E_{TM} \quad (1)$$

where  $E_{TM-CNC}$  are the total energies for TM-doped on surface reactivity of a CNC at the difference configurations. The  $E_{CNC}$  are the total energies of CNC with one vacancy carbon atom at doping site, while  $E_{TM}$  is a total energy of free

TM atom. A negative binding energy indicates that the system is an exothermic interaction.

### Partial charge transfers

Considering the partial charge transfer ( $Q_T$ ), the natural bond orbital (NBO) analysis was carried out to estimate the  $Q_T$ .<sup>17</sup> During the free metallic TM atom attacking on surface reactivity of the CNC, the  $Q_T$  is defined as a change of free metallic TM atom and TM charge during doping structures.

**Table 1.** Selected geometrical data of transition-doped CNC at the various doping configuration sites as computed at the B3LYP/LanL2DZ level.

Systems <sup>a</sup>	Bond length <sup>b</sup>						
	C1-C4	C1-C5	C1-C2	C2-C8	C2-C3	C3-C6	C3-C7
CNC	1.463	1.463	1.408	1.457	1.457	1.393	1.458
Sc-CNC(C1)	2.132	2.132	2.112	-	-	-	-
Ti-CNC(C1)	2.006	2.006	1.920	-	-	-	-
V-CNC(C1)	1.981	1.981	1.899	-	-	-	-
Cr-CNC(C1)	1.931	1.931	1.819	-	-	-	-
Mn-CNC(C1)	1.915	1.915	1.855	-	-	-	-
Sc-CNC(C2)	-	-	2.112	2.133	2.133	-	-
Ti-CNC(C2)	-	-	1.920	2.007	2.007	-	-
V-CNC(C2)	-	-	1.901	1.982	1.982	-	-
Cr-CNC(C2)	-	-	1.824	1.933	1.933	-	-
Mn-CNC(C2)	-	-	1.853	1.913	1.913	-	-
Sc-CNC(C3)	-	-	-	-	2.129	2.090	2.119
Ti-CNC(C3)	-	-	-	-	1.996	1.897	1.998
V-CNC(C3)	-	-	-	-	1.961	1.873	1.961
Cr-CNC(C3)	-	-	-	-	1.902	1.819	1.905
Mn-CNC(C3)	-	-	-	-	1.894	1.840	1.900

<sup>a</sup>Details of all systems were displayed in Figure 2. <sup>b</sup>In Å.

### Electronic properties

After the most stable structures with optimized geometries were obtained, all of relative species were subjected for further single point energy calculations. Mulliken electronegative ( $\chi$ ),

electronic chemical potential ( $\mu$ ), and chemical hardness ( $\eta$ ), known as chemical indices<sup>18</sup> for all CNC doped with a TM atom were computed using orbital energies of the highest occupied molecular orbital ( $E_{HOMO}$ ) and the lowest unoccupied



molecular orbital ( $E_{\text{LUMO}}$ ) at the B3LYP/LanL2DZ level of theory. These chemical indices,  $\chi$ ,  $\mu$ , and  $\eta$ , were derived from the first ionization potential (IP) and electron affinity (EA) of the  $N$ -electron molecular system with a total energy ( $E$ ) and external potential ( $v(\vec{r})$ ) using the relations:

$$\chi = -\left(\frac{\partial E}{\partial N}\right)_{v(\vec{r})} \quad (2)$$

$$\mu = -\frac{1}{2}(\text{IP} + \text{EA}) \quad (3)$$

$$\eta = \frac{1}{2}\left(\frac{\partial^2 E}{\partial N^2}\right)_{v(\vec{r})} \quad (4)$$

The  $\chi \approx -\mu$  and  $\eta \approx \frac{1}{2}(\text{IP} - \text{EA})$  are estimated for the electronegativity and the chemical hardness, respectively. The first IP and EA are computed using the formulae,  $\text{IP} = E(N-1) - E(N)$  and  $\text{EA} = E(N) - E(N+1)$ .<sup>19</sup> According to the Koopmans theorem,<sup>20</sup> IP and EA were computed from the HOMO and LUMO energies using the relations:  $\text{IP} = -E_{\text{HOMO}}$  and  $\text{EA} = -E_{\text{LUMO}}$ .

**Table 2.** Binding energy ( $E_b$ ), partial charge transfer ( $Q_T$ ), frontier molecular orbital energies, energy gaps ( $E_{\text{gap}}$ ), and chemical indices of transition-doped CNCs at the various doping configuration sites as computed at the B3LYP/LanL2DZ level.

Systems	$E_b^a$	$Q_T^b$	$E_{\text{HOMO}}^c$	$E_{\text{LUMO}}^c$	$E_{\text{gap}}^{c,d}$	$\eta^{c,e}$	$\mu^{c,f}$	$\chi^{c,g}$
CNC			-5.660	-3.184	2.476	1.238	-4.422	4.422
Sc-CNC(C1)	-176.59	1.551	-5.089	-3.782	1.306	0.653	-4.436	4.436
Ti-CNC(C1)	-224.95	1.154	-5.225	-3.102	2.123	1.061	-4.163	4.163
V-CNC(C1)	-207.27	0.858	-5.334	-2.884	2.449	1.225	-4.109	4.109
Cr-CNC(C1)	-201.74	0.561	-5.361	-3.510	1.850	0.925	-4.436	4.436
Mn-CNC(C1)	-193.18	0.618	-5.415	-2.966	2.449	1.225	-4.191	4.191
Sc-CNC(C2)	-169.87	1.549	-4.898	-3.701	1.197	0.599	-4.299	4.299
Ti-CNC(C2)	-217.96	1.148	-5.143	-3.048	2.095	1.048	-4.095	4.095
V-CNC(C2)	-201.05	0.858	-5.334	-2.912	2.422	1.211	-4.123	4.123
Cr-CNC(C2)	-196.21	0.563	-5.334	-3.456	1.878	0.939	-4.395	4.395
Mn-CNC(C2)	-187.62	0.609	-5.388	-2.939	2.449	1.225	-4.163	4.163
Sc-CNC(C3)	-135.78	1.532	-5.089	-3.755	1.333	0.667	-4.422	4.422
Ti-CNC(C3)	-187.43	1.136	-5.252	-3.075	2.177	1.088	-4.163	4.163
V-CNC(C3)	-172.27	0.810	-5.388	-3.021	2.367	1.184	-4.204	4.204
Cr-CNC(C3)	-168.56	0.514	-5.442	-3.429	2.014	1.007	-4.436	4.436
Mn-CNC(C3)	-157.78	0.591	-5.388	-2.939	2.449	1.225	-4.163	4.163

<sup>a</sup> In kcal/mol

<sup>b</sup> Defined as a change of adsorbate's charges during adsorption, in e.

<sup>c</sup> In eV.

<sup>d</sup>  $E_{\text{gap}} = E_{\text{LUMO}} - E_{\text{HOMO}}$ .

<sup>e</sup> Chemical hardness.

<sup>f</sup> Chemical potential.

<sup>g</sup> The Mulliken electronegativity.

Density of states (DOSs) for possible structures of all CNCs doped with TM atom were created from orbital energies which are contained in Gaussian output file. The total DOSs was calculated from the eigenvalues generated by single point calculations, as using the relations:

$$\text{DOS} = \sum_{i=1}^N \text{occ}(i) \exp\{-(E - C_i)^2\} \quad (5)$$

here  $N$  is the number of orbitals with a total energy  $E$ ,  $\text{occ}(i)$  is the number of occupation, and  $C_i$  is the vector of eigenvalues of the molecular orbitals. In all graphs the Fermi level was centered on the 0 value.<sup>21,22</sup>

## Results and discussion

### Geometrical structures, binding energies, and charge transfers

The B3LYP/LanL2DZ-optimized structures of Sc-, Ti-, V-, Cr-, and Mn-doped CNCs at the various doping configuration sites are displayed in Figure 2. The selected corresponding geometrical bond lengths of undoped and Sc-, Ti-, V-, Cr-, Mn-doped CNCs are listed in Table 1. The bond lengths observed in undoped CNC are C1-C4 (1.463 Å), C1-C5 (1.463 Å), C1-C2 (1.408 Å), C2-C8 (1.457 Å), C3-C6 (1.393 Å), and C3-C7 (1.458 Å). After doped structures, the geometrical structures of the CNC dramatically change due to the doping effect. Bond lengths of all TM-doped CNCs obtained in this study were elongated in comparison with undoped structures. Average bond lengths of TM-doped CNCs of 1.915–2.132

Å, 1.915–2.132 Å, 1.913–2.133 Å, 1.840–2.090 Å, and 1.900–2.119 Å for TM-C4, TM-C5, TM-C8, TM-C6, and TM-C7, respectively, were obtained.

To better understand the strong interactions between the TM atom and its three nearest carbon atoms at doping site that are solved in term of binding energy. Therefore, binding energies of Sc-, Ti-, V-, Cr-, and Mn-doped CNCs at the various doping configuration sites are listed in Table 2. The strong interaction of TM atoms to CNC was in the order: Ti-CNC(C1) ( $E_b = -224.95$  kcal/mol) > Ti-CNC(C2) ( $E_b = -217.96$  kcal/mol) > V-CNC(C1) ( $E_b = -207.27$  kcal/mol) > Cr-CNC(C1) ( $E_b = -201.74$  kcal/mol) > V-CNC(C2) ( $E_b = -201.05$  kcal/mol) > Cr-CNC(C2) ( $E_b = -196.21$  kcal/mol) > Mn-CNC(C1) ( $E_b = -193.18$  kcal/mol) > Mn-CNC(C2) ( $E_b = -187.62$  kcal/mol)  $\approx$  Ti-CNC(C3) ( $E_b = -187.43$  kcal/mol) > Sc-CNC(C1) ( $E_b = -176.59$  kcal/mol) > V-CNC(C3) ( $E_b = -172.27$  kcal/mol) > Sc-CNC(C2) ( $E_b = -169.87$  kcal/mol) > Cr-CNC(C3) ( $E_b = -168.56$  kcal/mol) > Mn-CNC(C3) ( $E_b = -157.78$  kcal/mol) > Sc-CNC(C3) ( $E_b = -135.78$  kcal/mol). This suggested that Ti atom exhibited the strongest interaction with CNC, while Sc atom exhibited the weakest interaction with CNC.

The data of  $Q_T$  of are also listed in Table 2. The values of  $Q_T$  of all various CNC doped with TM atoms were in the range of 0.514–1.551 e. The positive  $Q_T$  values, implied that the transferring direction of electron was from TM to CNC. This confirmed here that the strong binding interactions between TM atoms and CNC are occurred.

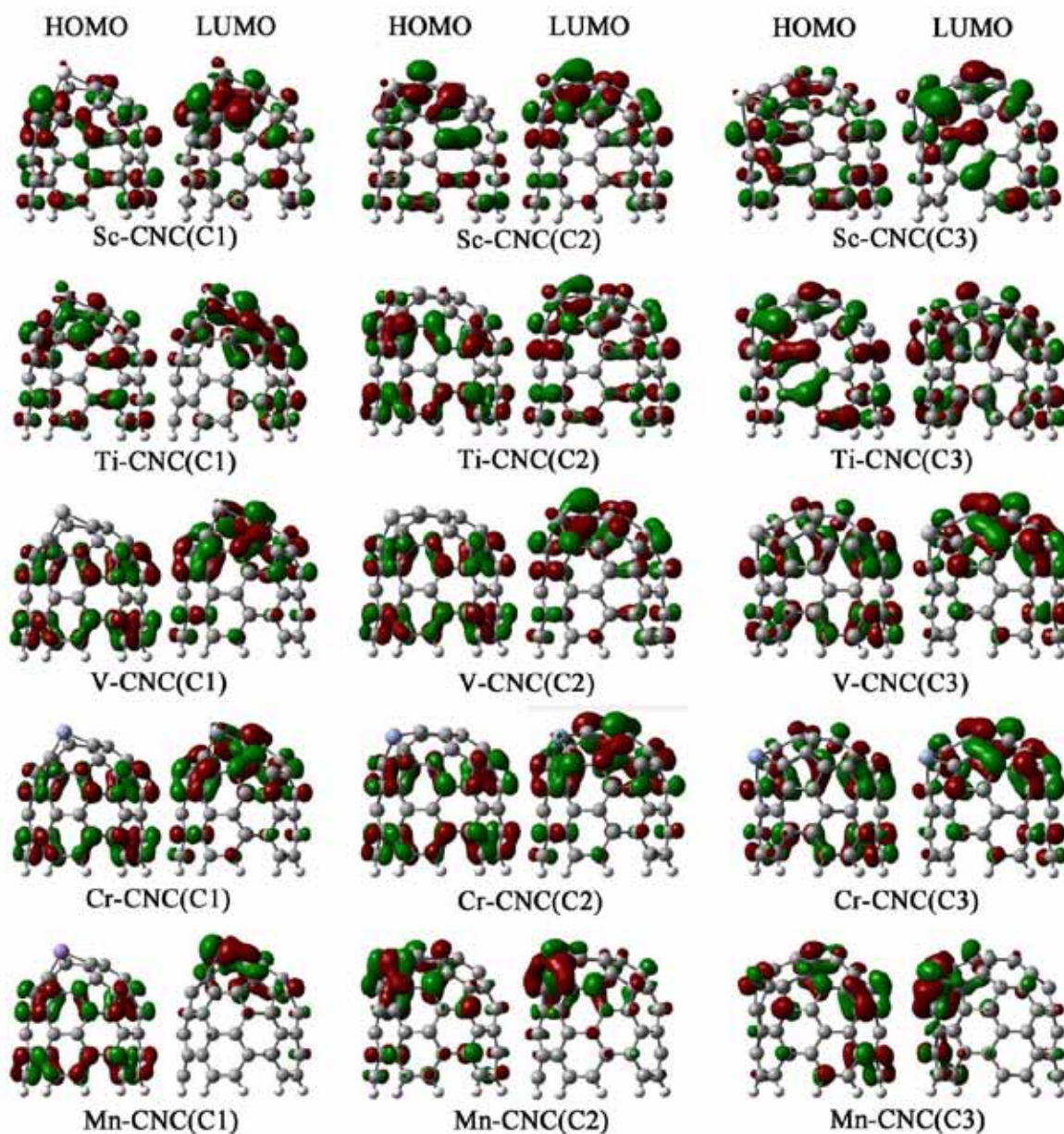


**Figure 4.** The frontier molecular orbitals of transition-doped CNCs at the various doping configuration sites as computed at the B3LYP/LanL2DZ level.

### Electronic properties

To investigate the electronic properties, the frontier molecular orbital energies, energy gaps, and chemical indices of undoped and Sc-, Ti-, V-, Cr-, Mn-doped CNCs are also computed and listed in Table 2. In general, the gaps between HOMO and LUMO are important tools to study the stability and conductivity of the complexes. The

undoped CNC structure which energy gap of 2.476 eV, showed the semi-conductive behavior.<sup>22</sup> The values of  $E_{\text{gap}}$  of TM-doped CNCs were in the range of 1.197–2.449 eV, suggested that the gap was narrowed when comparing to undoped structure. However, the chemical indices are important tools to study the stabilities of these complexes. According to the Koopmans theorem,<sup>20</sup> the chemical hardness, electronic



chemical potential, and Mulliken electronegativity of all TM-doped CNCs were changed when comparing to undoped CNC.

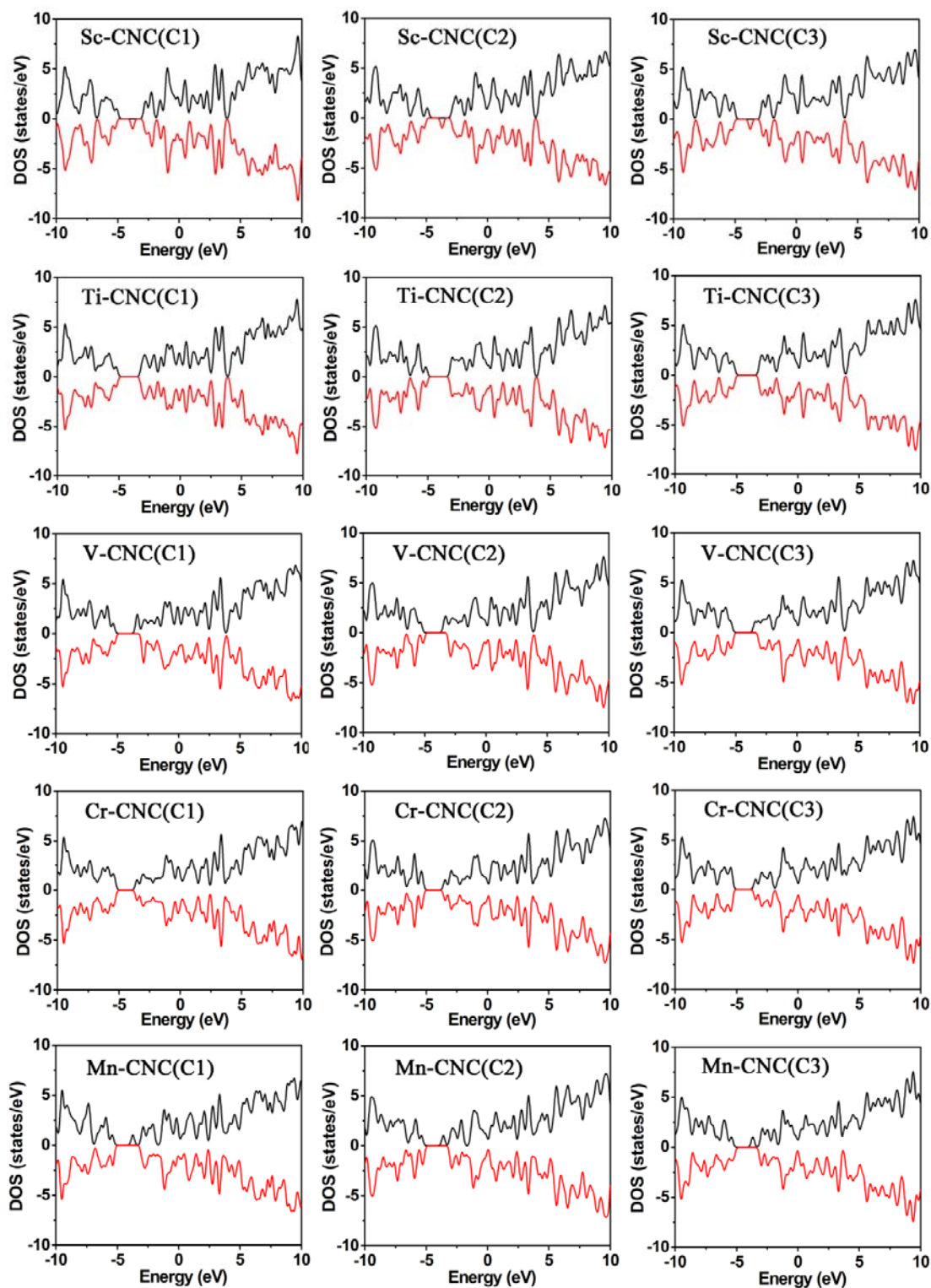


**Figure 5.** The density of states of transition-doped CNCs at the various doping configuration sites as computed at the B3LYP/LanL2DZ level.



The frontier molecular orbitals and DOS of undoped CNC are displayed in Figure 3. The plots of the HOMO and LUMO of undoped CNC showed that electron densities were vicinity around the cap. Furthermore, the plots of frontier molecular orbitals of Sc-, Ti-, V-, Cr-, and Mn-doped CNCs at the various doping configuration sites are displayed in Figure 4. The electron densities of HOMOs were mostly located around the cap, except in Sc-CNC(C2) and Mn-CNC(C2) which were located on dopants. However, the electron densities of LUMOs were delocalized to the dopants. This suggested that the metals bound strongly with CNC to minimize its structural energy.

The electronic DOSs of Sc-, Ti-, V-, Cr-, and Mn-doped CNC at the various doping configuration sites are displayed in Figure 5. The DOSs of the TM-doped CNCs displayed both different symmetrical and asymmetrical patterns and band gaps. The symmetrical peaks of the spin up and spin down of singlet-electron were obtained from Ti and Cr atoms. In contrast, The asymmetrical peaks of the spin up and spin down of doublet-electron were obtained from Sc, V, and Mn atoms. It is apparent that the DOSs of Sc-, V-, and Mn-doped CNTs were asymmetries while the DOSs of Ti- and Cr-doped CNTs were symmetries. After doping with atoms, the DOSs introduced that the filling electronic states of the dopant TM atom into the undoped CNC induced the narrower band gaps, suggesting that the CNC changed its electronic property nearly to approach a conductor.<sup>22</sup>

## Conclusion

The structure, energy, charge transfer, and electronic properties of CNC doping with TM atom Sc, Ti, V, Cr, and Mn were studied using the DFT

method. Calculated results showed that after doped structures, the geometrical structures of the CNC dramatically change at the doping site to form the pyramidal shape. The gaps between HOMO and LUMO are important tool to study the stabilities of these complexes. The undoped CNC structure which has the energy gap of 2.476 eV, displayed the semi conductive behavior. In the TM-doped-CNCs, the values of  $E_{\text{gap}}$  were decreased to the range of 1.197–2.449 eV, suggesting that energy gaps were narrowed in comparion with undoped structure. In addition, the binding ability indicated that Ti atom exhibited the strongest interaction with CNC, while Sc atom exhibited the weakest interaction with CNC. This is consistent with the transferring direction of electron from TM to CNC. Furthermore, the frontier molecular orbitals of electron densities of TM-doped CNCs were delocalized to the dopants. This suggested that the metals bound strongly with CNC to minimize its structural energy. In addition, the DOSs of the TM-doped CNCs displayed both different symmetrical and asymmetrical patterns and band gaps.

## Acknowledgments

This work is kindly thanks to the Project Teachers with Special Knowledge in the institute for the promotion of teaching science and technology (IPST)for financial support. Also, the work is gratefully acknowledged to Center of Excellence for Innovation in Chemistry and Supramolecular Chemistry Research Unit, Department of Chemistry, Faculty of Science, Mahasarakham University for providing facilities.

## References

- Iijima S. Helical microtubules of graphitic carbon. *Nature* 1991; 354:56–58.
- Su Y, Yang Z, Wei H, Kong E.S, Zhang Y. Synthesis of single-walled carbon nanotubes with selective diameter distributions using DC arc discharge under CO mixed atmosphere. *Appl. Surf. Sci.* 2011; 257:3123–3127.
- Rinkiö M, Johansson A, Paraoanu G.S, Törmä P. High-speed memory from carbon nanotube field-effect transistors with high-*K* gate dielectric. *NanoLett.* 2009; 9:643–647.
- Zhou X, Tian W.Q, Wang X. Adsorption sensitivity of Pd-doped SWCNTs to small gas molecules. *Sens. Actuators B: Chem.* 2010; 151:56–64.
- Shalabi A.S, Abdel Aal S, Assema M.M, Abdel Halim W.S. Ab initio characterization of Ti decorated SWCNT for hydrogen storage. *Int. J. Hydrogen Energy* 2013; 38: 140–152.
- Park S, Park S, So H, Jeon E, Park D, Kim J, Kim B.S, Kong K, Chang H, Lee J. Computer-aided design and growth of single-walled carbon nanotubes on 4 in. wafers for electronic device applications. *Carbon* 2010; 48:2218–2224.
- Yeung C.S, Liu L.V, Wang Y.A. Adsorption of small gas molecules onto Pt-Doped single-walled carbon nanotubes. *J. Phys. Chem. C* 2008; 112:7401–7411.
- Tabtimsai C, Keawwangchai S, Wannob, Ruangpornvisuti V. Gas adsorption on the Zn-, Pd- and Os-doped armchair (5,5) single-walled carbon nanotubes. *J. Mol. Model.* 2012; 18: 351–358.
- Tabtimsai C, Keawwangchai S, Nunthaboot N, Wannob, Ruangpornvisuti V. Density functional investigation of hydrogen gas adsorption on Fe-doped pristine and stone-wales defected single-walled carbon nanotubes. *J. Mol. Model.* 2012; 18:3941–3949.
- Chen Y.K, Liu L.V, Tian W.Q, Wang Y.A. Theoretical studies of transition-metal-doped single-walled carbon nanotubes. *J. Phys. Chem. C* 2011; 115:9306–9311.
- Yeung C.S, Wang Y.A. Lewis Acidity of Pt-doped buckybowls, fullerenes, and single-walled carbon nanotubes. *J. Phys. Chem. C* 2011; 115:7153–7163.
- Yu X, Zhang J, Choi W, Choi J, Kim J.M, Gan L, Liu Z. Cap formation engineering: from opened C<sub>60</sub> to single-walled carbon nanotubes. *NanoLett.* 2010; 10:3343–3349.
- Frisch M.J, et al., Gaussian09, revision B.01, Gaussian Inc, Wallingford CT, 2009.
- Becke A.D. Density-functional exchange-energy approximation with correct asymptotic behavior. *Phys. Rev. A* 1988; 38:3098–3100.
- Lee C, Yang W, Parr R.G. Development of the colic-salvetti correlation-energy formula into a functional of the electron density. *Phys. Rev. B* 1988; 37:785–789.
- Hay P.J, Wadt W.R. Ab initio effective core potentials for molecular calculations. Potentials for K to Au including the outermost core orbitals. *J. Chem. Phys.* 1985; 82:270–283.
- Reed A.E, Curtiss L.A, Weinhold F. Intermolecular interaction from a natural bond orbital, donor-acceptor viewpoint. *Chem. Rev.* 1988; 88:899–926.
- Parr R.G, Szentpály L.V, Liu S. Electrophilicity index. *J. Am. Chem. Soc.* 1999; 121:1922–1924.
- Sabin J.R, Trickey S.B, Apell S.P, Oddershede J. Molecular Shape, Capacitance, and Chemical Hardness. *Int. J. Quantum Chem.* 2000; 77:358–366.



20. Koopmans T. Über die zuordnung von wellenfunktionen und eigenwertenzu den einzelnenelektroneneinesatoms. *Physica* 1934; 1:104–113.
21. Gómez B, Martínez–Magadán J.M. A theoretical study of dibenzothiophene adsorbed on open-ended carbon nanotubes. *J. Phys. Chem. B* 2005; 109:14868–14875.
22. Tabtimsai C, Tontapha S, Rakrai W, Wannob. A DFT study on structural stability and electronic property of VIII B transition metal-doped carbon nanocaps. *Sol. State Sci.* 2014; 37:6–12.